# Allosteric changes of the NMDA receptor trap diffusible dopamine 1 receptors in spines

**Lena Scott*, Sergey Zelenin*, Seth Malmersjö*, Jacob M. Kowalewski†, Eivor Zettergren Markus*, Angus C. Nairn‡§, Paul Greengard§, Hjalmar Brismar*†, and Anita Aperia*¶**

*Department of Woman and Child Health, Karolinska Institutet, Astrid Lindgren Children's Hospital Q2:09, S-171 76 Stockholm, Sweden; †Department of Cell Physics, Royal Institute of Technology, S-106 91 Stockholm, Sweden; ‡Department of Psychiatry, Yale University School of Medicine, New Haven, CT 06519; and §Laboratory of Molecular and Cellular Neuroscience, The Rockefeller University, New York, NY 10021-6399

Edited by Richard L. Huganir, The Johns Hopkins University School of Medicine, Baltimore, MD, and approved November 18, 2005 (received for review July 1, 2005)

**The dopaminergic and glutamatergic systems interact to initiate and organize normal behavior, a communication that may be perturbed in many neuropsychiatric diseases, including schizophrenia. We show here that NMDA, by allosterically modifying NMDA receptors, can act as a scaffold to recruit laterally diffusing dopamine D1 receptors (D1R) to neuronal spines. Using organotypic culture from rat striatum transfected with D1R fused to a fluorescent protein, we show that the majority of dendritic D1R are in lateral diffusion and that their mobility is confined by interaction with NMDA receptors. Exposure to NMDA reduces the diffusion coefficient for D1R and causes an increase in the number of D1R-positive spines. Unexpectedly, the action of NMDA in potentiating D1R recruitment was independent of calcium flow via the NMDA receptor channel. Thus, a highly energy-efficient, diffusion-trap mechanism can account for intraneuronal interaction between the glutamatergic and dopaminergic systems and for regulation of the number of D1R-positive spines. This diffusion trap system represents a molecular mechanism for brain plasticity and offers a promising target for development of antipsychotic therapy.**

organotypic cultures | fluorescence recovery after photo-bleaching | lateral diffusion | receptor movement

A variety of pharmacological, biochemical, and molecular genetic evidence indicates that the schizophrenic state is associated with hypoglutamatergia and a high ratio of D2 dopaminergic to D1 dopaminergic signaling (1, 2). We recently reported a cellular interaction between NMDA receptors and D1 receptors (D1Rs) that can explain how such abnormalities in glutamate and dopamine signaling might be causally related. Specifically, activation of NMDA receptors was shown to increase recruitment of D1Rs but not of D2Rs in the plasma membrane of primary cultures of striatal neurons (3). In view of the potential clinical relevance of NMDA-induced selective recruitment of dopamine D1Rs, we have, in the present study, explored the underlying mechanism. Here, we provide evidence that dopamine D1Rs, laterally diffusing in the dendritic plasma membrane, can be trapped in spines by ligand-occupied NMDA receptors.

## Results

To monitor its mobility in live neurons, the D1R was tagged with the fluorescent protein Venus (D1R-Venus) (4) and expressed in organotypic cultures from rat striatum (Fig. 1*a*). The fluorescent signal was evenly distributed in the cell body and plasma membrane. A strong signal was also recorded from the dendritic tree (Fig. 1*b*). Approximately five D1R-positive spines were detected per 10 $\mu$m of dendrite. D1R-positive spines were mushroom shaped, thin, or stubby. Filopodia-like D1R-positive structures were rare. The subcellular distribution of D1R-Venus was similar to that described in electron microscope studies of endogenous D1R (5, 6). No distinct D1R signal was observed in glial cells. This lack of signal from glial cells minimized the background signal and made this study feasible (Fig. 1*c*). The selective distribution of the D1R-Venus signal in neurons was observed after both biolistic and viral transfection of D1R (the latter method was used in a few pilot studies).

Medium spiny neurons in the corticostriatal region are regulated by a major glutamatergic corticostriatal projection and by a dopaminergic nigrostriatal projection. In these medium spiny neurons, D1R and NMDA receptors are known to interact (7). Brief exposure (30 s, followed by 15 min wash out) of organotypic striatal cultures to NMDA caused an increase in D1R-positive spines. An area containing part of the dendritic tree was magnified to visualize spines. Analysis of the same area was made before and after exposure to NMDA (Fig. 2*a*). By examining a large 3D stack of images, small changes in focus and movement of dendrites could be compensated for. In pilot studies, we observed an increase in D1R-positive spines after 3 min. The increase reached a plateau between 10 and 15 min after NMDA exposure, and a second recording was made during this time period. At that second recording, a significant (21 $\pm$ 4%) increase in the number of WT D1R-positive spines was observed. Eleven dendrites were studied before and after NMDA exposure, and, in each case, an increase in number of spines was found (Fig. 2*b*). Activation of NMDA receptors in hippocampal neurons has been shown to cause out-growth of filopodia-like protrusions from the dendritic tree within 30 min of exposure (8). Most of these structures will later develop into spines. We observed very few D1R-positive filopodia-like structures. To exclude the possibility that the effects we recorded were due to an increase in the total number of spines rather than to an increase in the number of D1R-positive spines, filopodia-like structures were not included in our calculations. In control experiments using neurons transfected with soluble Venus protein, we did not observe an increase in the number of spines 15 min after NMDA exposure.

The ratio between plasma membrane (m) and cytosolic (c) D1R-Venus signal in cell body was, during control conditions, 0.90 $\pm$ 0.02. After 30 s exposure to NMDA, the m/c ratio was increased to 1.15 $\pm$ 0.04 ($P < 0.05$ vs. control); after 15 min washout, the m/c ratio had returned to control level, 0.88 $\pm$ 0.02. These findings are in line with our observations in a previous study where an immunocytochemical technique was used to examine the subcellular localization of D1R (3). The ratio between plasma membrane and cytosolic D1R-Venus signal in dendrites was not found to be different before and after NMDA exposure (1.10 $\pm$ 0.02 vs. 1.06 $\pm$ 0.02).

To explore the mechanism of D1R movement in the dendritic tree, the fluorescence signal was photo-bleached, and the fluo-

Conflict of interest statement: No conflicts declared.

This paper was submitted directly (Track II) to the PNAS office.

Abbreviations: D1R, D1 receptor; FRAP, fluorescence recovery after photo-bleaching.

¶To whom correspondence should be addressed. E-mail: anita.aperia@kbh.ki.se.





www.pnas.org/cgi/doi/10.1073/pnas.0505557103

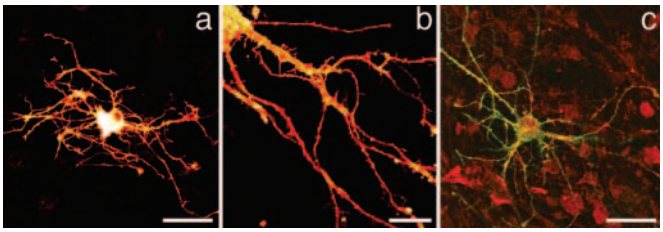


**Fig. 1.** Expression of D1R-Venus in organotypic cultures. (*a*) Fluorescence image of a neuron in striatal organotypic culture expressing D1R-Venus. (Scale bar: 50 $\mu$m.) (*b*) The image shows extended focus projection from several confocal sections of a neuron. The signal was optimized for imaging of thin dendritic structures. (Scale bar: 20 $\mu$m.) (*c*) Image of a neuron expressing D1R-Venus (green); the signal was optimized to visualize the underlying nontransfected glia cells (red) in the culture. (Scale bar: 50 $\mu$m.)

rescence recovery after photo-bleaching (FRAP) was recorded. Dendrites that closely paralleled the image plane were selected for FRAP analysis. Dendrites are, due to their simple geometry, excellent targets for FRAP experiments. They are thin, allowing for complete bleach through their entire cross section, and they can be modeled as a tube for analysis of diffusion parameters. We used dendritic segments before the first branching and at a distance of 50–150 $\mu$m from the cell body. The recovery pattern for D1R is illustrated in Fig. 3*a* and in Movie 1, which is published as supporting information on the PNAS web site. The recovery pattern could be described by the solution for the diffusion equation in a tube (see *Supporting Text* and Figs. 8 and 9, which are published as supporting information on the PNAS web site) based on Fick's second law. Maximal recovery occurred within the first 4 min after bleaching. The initial signal was recovered to 64 ± 10%, indicating that the majority of D1R belong to a mobile fraction. This mobile pool fulfilled several of the criteria for lateral diffusion: the recovery curve fits to the general equation for diffusion, recovery occurred symmetrically

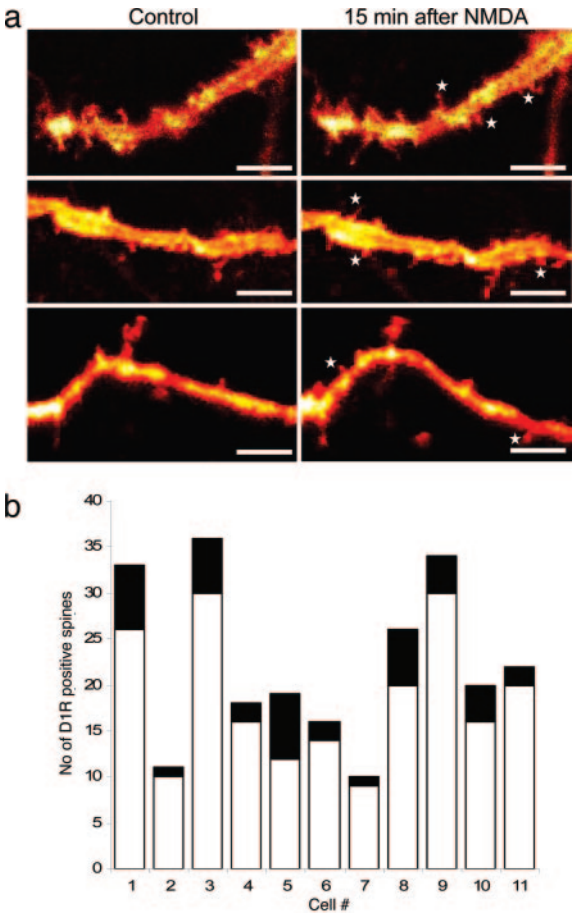


**Fig. 2.** Number of D1R positive spines before and after NMDA exposer. (*a*) Magnification of a segment of a dendritic tree expressing D1R-Venus. Asterisks indicate new D1R-positive spines after NMDA treatment. (Scale bar: 10 $\mu$m.) (*b*) Spines were counted 10–15 min after terminating exposure to NMDA ($10^{-3}$ M for 30 s). D1R-positive spines under control conditions are indicated by the open parts of the bars; additional D1R-positive spines after NMDA exposure are indicated by the filled parts of the bars.

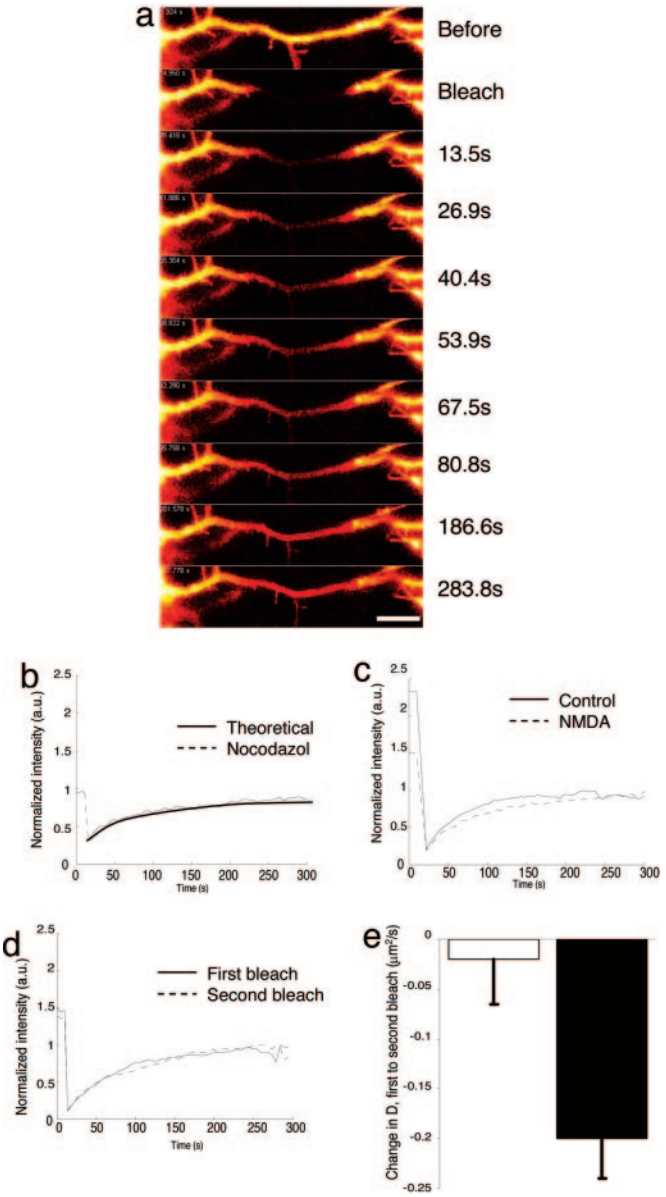


**Fig. 3.** Lateral diffusion of D1R studied with FRAP. (*a*) Representative time series from a FRAP experiment. (Scale bar: 10 $\mu$m.) (*b*) Fluorescence recovery after disruption of microtubules by nocodazole ($10^{-4}$ M, 20-min treatment before recording). (*c*) Treatment with NMDA (dashed line, $10^{-3}$ M) reduces fluorescence recovery rate. Similar results were found for $10^{-5}$ M, $10^{-4}$ M, and $10^{-3}$ M NMDA. (*d*) Fluorescence recovery rate after repeated bleaching sessions. solid line, first bleach; dashed line, second bleach. (*e*) Change in diffusion coefficient between first and second bleach (open bar) before and after exposure to NMDA, $10^{-3}$ M (filled bar), $n = 5$.

NEUROSCIENCE

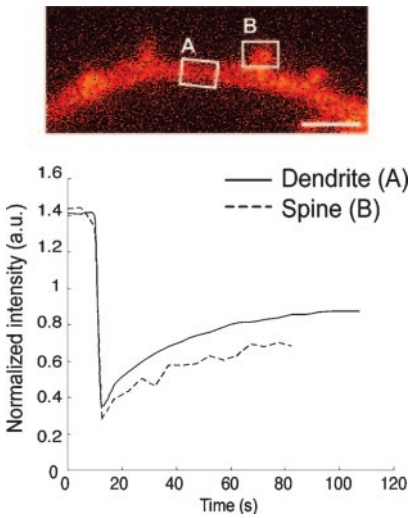


**Fig. 4.** The fluorescence recovery of D1R signal in spines. Bleaching was performed on a D1R-positive spine (area B and dashed line) and, for control purpose, on an equally sized segment of the dendrite (area A and solid line) in the same field of view. (Scale bar: 2 $\mu$m.) The fluorescence recovery was slower in spines than in the dendrite segment.

from both ends of the bleached region, and the fluorescent signal was homogenous and not punctuate (Fig. 3*a*). In control cells, the mean apparent diffusion coefficient was 0.70 ± 0.06 $\mu m^2/s$ ($n$ = 16), which is somewhat higher than that suggested by Choquet and Triller (9) as typical for movement within a lipid membrane. Their studies were performed in a nanoscale, with attention paid to the fact that the lipid membrane is made up of a mosaic of lipid platforms. The FRAP technique, which is well suited for studies of how a physiological or pharmacological stimulus may alter the diffusion of a protein, measures the bulk of D1R movement in dendritic shafts and spines and provides an average value for the apparent diffusion coefficient in these different platforms.

Our data are not compatible with the notion that vesicular transport is the predominant pathway for D1R movement in dendrites. If the major fraction of mobile D1R were located in vesicles and transported along microtubules, the fluorescent recovery would not fit with the diffusion equation. Furthermore, nocodazole, used to disrupt microtubules (Fig. 3*b*), had no effect on the pattern of the recovery. Taken together, our data strongly indicate that a large fraction of D1R in the dendritic shaft diffuses in the plasma membrane. This finding raises the question of whether the recruitment of D1R to spines is achieved by a diffusion-trap mechanism. If so, NMDA activation would be expected to reduce the rate of D1R diffusion. As shown in Fig. 3 *c* and *e*, this was found to be the case. To test the effect of NMDA exposure, two separate bleach and recording sessions were made from the same area. The first recording was made under control conditions. The cells were then exposed to NMDA for 30 s, and the second bleach and recording session was performed 3 min after the exposure. NMDA exposure caused a significant (0.20 ± 0.04 $\mu m^2/s$) decrease of diffusion coefficient ($n$ = 16, $P < 0.001$). To control for possible effects of repeated photo-bleaching, two bleach and recording sessions were performed under control conditions. No effect of repeated photobleaching on the recovery rate was found (Fig. 3*d*).

In spines, NMDA receptors are generally firmly anchored to the postsynaptic density. An association between D1R and the NR-1 subunit of the NMDA receptor has been shown to exist in the postsynaptic density (7). We next performed a study where bleaching was performed on a D1R-positive spine and, for control purposes, on an equally sized segment of the dendrite in the same field of view (Fig. 4). The apparent diffusion coefficient was significantly lower (51% ± 4%, $n$ = 4, $P < 0.05$) in spines than in the dendrite segment, indicating a larger resistance to random movement. This finding is compatible with the concept that D1R is preferentially trapped in spines.

A direct interaction has been demonstrated, between D1R and NMDA receptors, that is mediated by the binding of different regions of the C-terminal tail of D1R to either the NR1 or NR2 NMDA receptor subunit (10). We next asked whether the C-terminal tail of D1R carries information related to its local-

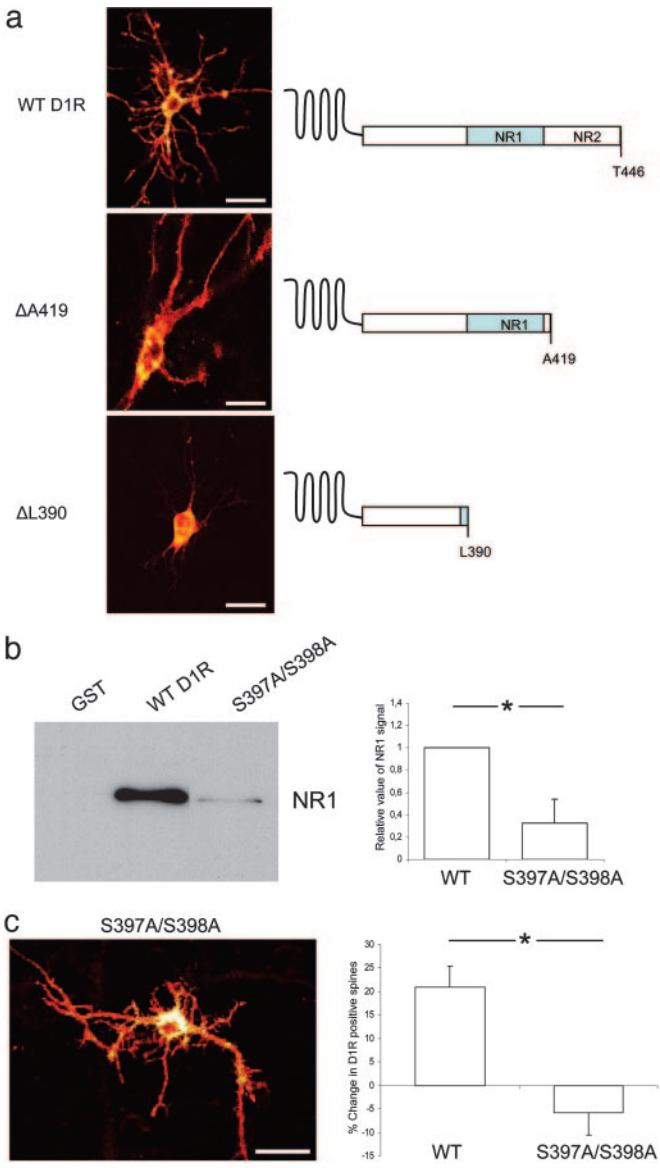


**Fig. 5.** Role of D1R C terminus on receptor localization and binding to NR-1. (*a*) Representative confocal images of neurons transfected with WT D1R, ΔA419, or ΔL390, fused to Venus. Truncation of the C terminus and binding sites for NMDA receptor subunit NR1 (L387–L416) and NR2A (S417–T446) are indicated. (Scale bar: 50 $\mu$m.) (*b*) Western blot of NR1 subunit after GST pull-down from rat striatal lysate using WT GST-D1R-L387-L416 (WT) or -S397A/S398A, or GST alone. The immunoblots were analyzed by using densitometry, and quantitation is shown in the bar graph (*, $P < 0.01$). (*c*) Confocal image of striatal organotypic neuron transfected with D1R-S397A/S398A. The bar graph compares the percentage change in D1R-positive spines in response to NMDA treatment for neurons expressing WT D1R (WT) or D1R-S397A/S398A (*, $P < 0.001$). (Scale bar: 50 $\mu$m.)

ization in dendrites and dendritic spines. To address this question, we truncated the C terminus at A419 (ΔA419, deletion of most of the NR2-binding region) and L390 (ΔL390, deletion of most of both NR1- and NR2-binding domains) (Fig. 5*a*). The localization of the ΔA419 protein in the cell body and dendritic tree was similar to that observed for WT D1R. There was also no apparent difference in the number of spines labeled by the ΔA419 and WT D1R proteins (data not shown). The signal for the ΔL390 protein was strong in the cell body but weak in dendrites and absent from spines. In HEK cells transfected with D1R and NMDA receptor, NMDA-triggered trafficking of D1R was reported to be inhibited by a peptide encompassing the NR-1-binding region of the D1R C terminus (10, 11) (residues 397–416, see Fig. 5*a*). In support of the importance of this region of D1R in binding to NR1, we found that combined mutation of S397 and S398 (both to alanine, S397A/S398A) significantly decreased binding to NMDA receptors, as demonstrated by a GST-pull down assay using GST-D1R-L387-L416 (Fig. 5*b*). A mutant D1R containing the S397A/S398A mutations was fused with the Venus fluorescent protein and transfected into organotypical striatal cultures. The fluorescent signal from cell body, dendritic tree, and spines seemed similar to that observed for WT D1R. However, addition of NMDA failed to increase the number of D1R-S397A/S398A-positive spines (Fig. 5*c*). Nor was the apparent diffusion coefficient for the D1R-S397A/S398A significantly changed (Δ diffusion coefficient = 0.05 ± 0.02 $\mu m^2/s$, $n = 6$) after NMDA exposure, in FRAP experiments of the dendritic shaft. These results suggest that direct interaction between D1R and NMDA receptors is required for NMDA-triggered trapping of D1R. S397 and S398 are potential targets for phosphorylation by CK1, CK2, and perhaps PKC and CaM-kinase. However, CK1, CK2, PKC, and CaM-kinase II did not phosphorylate these sites in the purified L387-L416 fusion protein (K. Sugimoto, A.C.N., and A.A., unpublished results).

We next addressed the question of whether allosteric effects on the NMDA receptor caused by ligand binding may, without activation of an intracellular calcium-signaling pathway, enhance NMDA and D1R interaction and trigger trapping of D1R. The NMDA receptor channel is a tetrameric protein composed of NR1 and at least one of the NR2 subunits A–D. The receptor has two physiological ligands, glutamate and glycine. The binding sites for glutamate and glycine seem to be distinctly separate sites (12, 13). NMDA is a potent agonist acting at the glutamate-binding site. Activation of either site increases calcium permeability of the NMDA receptor channel. To investigate whether the effect of the NMDA receptor on D1R mobility is mediated by means of calcium influx, we added NMDA together with magnesium, because magnesium is known to block the channel. This procedure resulted in a similar increase of D1R-positive spines compared with addition of NMDA alone (Fig. 6 *a* and *b*). Next, we added glycine in the absence of magnesium (Fig. 6 *a* and *b*). No increase in D1R-positive spines was observed. In control assays, NMDA or glycine did, in the absence of magnesium, cause an increase of intracellular calcium (Fig. 6*c*).

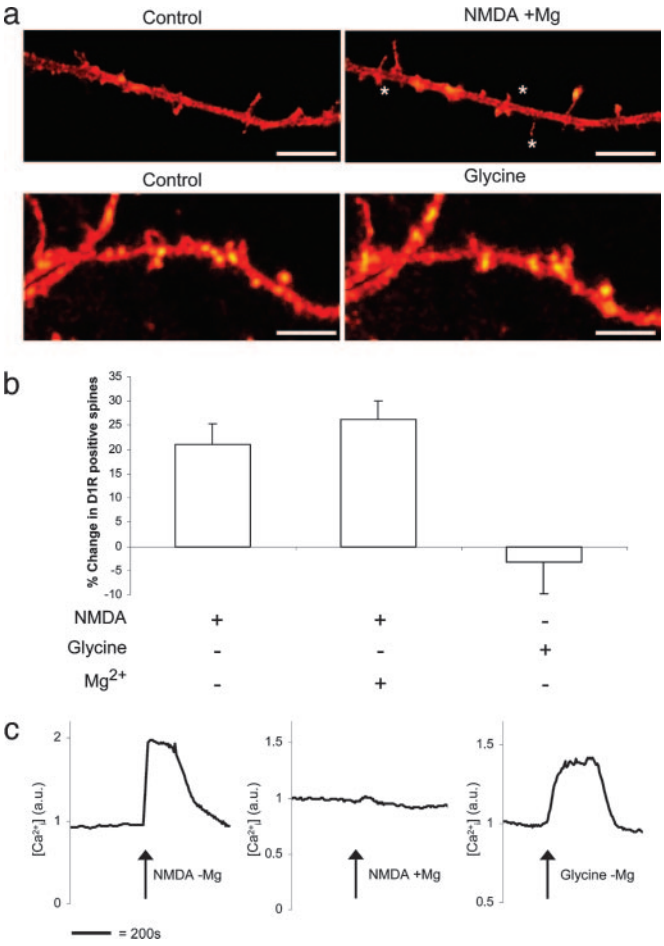


**Fig. 6.** Effects of NMDA and glycine on calcium flux and D1R trapping. (*a*) Magnification of segments of dendrites. Cells were treated with either NMDA ($10^{-3}$ M) plus $Mg^{2+}$ or with glycine ($2 \times 10^{-3}$ M) for 30 s, followed by a 15-min washout. Asterisks indicate new D1R-positive spines after treatment. (Scale bar: 10 $\mu$m.) (*b*) Bar graph shows percentage change of D1R-positive spines in response to treatment condition indicated. (*c*) Intracellular calcium levels measured in response to treatment with NMDA ($10^{-3}$ M) in the absence (−Mg) or presence (+Mg) of magnesium, and to glycine ($2 \times 10^{-3}$ M) in the absence of magnesium (−Mg).

## Discussion

The concept that lateral diffusion of receptors in the plane of the membrane can regulate receptor stabilization at synapses originally emerged from studies of acetylcholine receptors (14, 15). More recently, studies by Triller and Choquet (16) have shown that lateral diffusion of receptors is, in addition to endo-/exocytotic processes, a major mechanism for receptor accumulation at synapses. Despite the enormous importance of the dopaminergic system, little has been known about the mechanisms by which D1Rs are localized in dendrites.

Here, we show that lateral diffusion is a major pathway for localization of D1R in spines and that the diffusible pool of D1R plays an important role for the intraneuronal interaction between the dopaminergic and the glutamatergic systems. Trapping of diffusing receptors is postulated to result from their interactions with submembranous scaffolding proteins. Thus, gephyrin will confine the movement of glycine receptors, resulting in the temporary stabilization of these receptors in synapses (16, 17). The metabotropic glutamate receptors are confined to synapses by means of interaction with the homer protein (18). Trapping of D1R was found in the present study to occur after interaction with a ligand-gated ion channel. This interaction was independent of calcium flow via the NMDA receptor and instead seemed to be triggered by allosteric modification of the NMDA receptor. The major concept of the allosteric theory of signal transduction is that receptors exist in an equilibrium of conformational states. After ligand binding, one conformation of the receptor is stabilized, shifting the equilibrium toward this state (19). Our data indicate that occupation of the NMDA-binding site of the NMDA receptor favors a conformation that will bind to D1R and stabilize D1R in spines.

NMDA receptors are, according to several recent reports, targeted to spines both via vesicular transport and via lateral movement in the plasma membrane (20). The NMDA receptor is anchored to the postsynaptic density via several proteins,

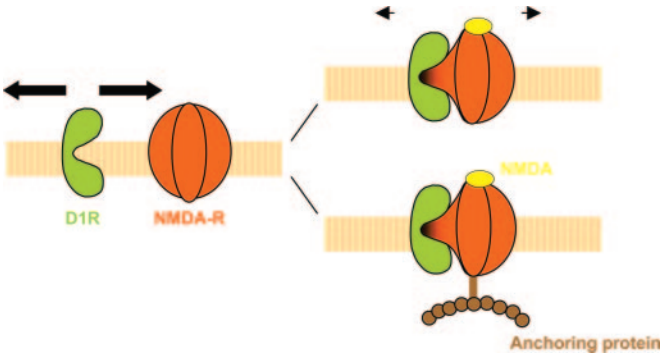


**Fig. 7.** Schematic drawing of D1R movement. D1R randomly diffuses in the plasma membrane and can physically interact with NMDA receptors (NMDA-R), which have undergone an allosteric change, due to ligand occupation of the NMDA/glutamate-binding site. Formation of a D1R–NMDA receptor complex reduces D1R mobility. When the NMDA receptor is anchored to postsynaptic density, movement is arrested.

including actin and PSD-95 (21, 22). A picture (Fig. 7) now emerges for how NMDA receptor activation can modulate the localization of D1R in dendrites and spines. A large reservoir pool of D1R randomly diffuses in the plasma membrane of dendrites. D1R and NMDA receptors can interact physically, and this interaction is enhanced by the allosteric effect of ligand occupation of the NMDA/glutamate-binding site of the NMDA receptor. Formation of D1R–NMDA receptor complexes slows down diffusion. The plasma membrane of the dendritic shaft and the spine probably represents a continuum. Because NMDA receptors are firmly anchored to the postsynaptic density, formation of D1R/NMDA receptor complexes is likely to stabilize D1R in spines, and NMDA exposure was indeed found to increase the number of D1R-positive spines. The D1R/NMDA receptor complexes may either be transported to, or formed in, the spines. The described mechanism for D1R accumulation in spines is highly energy-efficient, because it depends on diffusion and receptor allosterism. The integration of the dopaminergic and glutamatergic systems plays a key role in the plasticity of normal and abnormal behavior (23). The diffusion-trap system, by which allosteric modification of the glutamatergic NMDA receptor can trigger the recruitment of dopamine 1 receptors to neuronal spines, represents a molecular mechanism for brain plasticity and offers a promising target for development of antipsychotic therapies.

## Methods

**Neuronal Cultures.** Striatal organotypic cultures were prepared from 5- to 6-day-old Sprague–Dawley rats, according to Wray (24), by using DMEM and Hank's balanced salt solution (1.55:1). The cultures were grown in the presence of 0.297% glucose, 0.01 M Hepes, 10% fetal calf serum (FBS) and 1% antibiotic-antimycotic. Cultures were kept in a roller drum at 37°C at an approximate humidity of 95–98% with a $CO_2$ concentration of 5%, and grown for 21 days before experiments were performed. Striatal primary cultures were prepared as described by Tang and Bezprozvanny (25) with the following modifications: 10% FBS was used instead of heat-inactivated FBS, and 5 $\mu$M cytosine arabinoside was added at day 4–6 days *in vitro*.

**D1R Constructs.** cDNA fragment-coding full-length rat D1R (accession number NP_036678) was cloned into pVenus-N3 vector (pD1R-Venus) with a CMV promotor. pD1R-Venus was modified to obtain a mutant cDNA encoding rat D1R with truncation at A419 ($\Delta$A419) or L390 ($\Delta$L390), and a mutant where serine 397 and serine 398 were replaced with alanine, S397A/S398A. A construct encoding GST-fusion protein with D1R C-terminal residues CT L387–L416, was cloned in a pDEST15 vector by using site-specific recombination (Gateway Technology, Invitrogen). The full-length or fragment of rat D1R C terminus cDNA was mutated at amino acid positions S397/S398 by a site-directed mutagenesis technique by using the U.S.E. Mutagenesis Kit (Amersham Pharmacia). Structure of all constructs was confirmed by DNA sequencing.

**GST Affinity Pull-Down.** GST affinity pull-down was used to study the interaction between the NMDA receptor and two peptide segments corresponding to the C terminus tail of D1R. GST fusion proteins were produced in *Escherichia coli* (BL21-A1) and purified by using glutathione Sepharose 4B beads (Amersham Pharmacia Biosciences). Rat striatal lysate was prepared in lysis buffer containing 50 mM Tris·HCl, 150 mM NaCl, 2 mM EDTA, 1 mM phenylmethylsulfonyl fluoride, 0.25% sodium deoxycholate, 1% Triton X-100, and protease inhibitors. Striatal lysate (50 $\mu$g of total protein) was added to the beads in a volume of 1 ml and incubated overnight at +4°C. Samples were separated by SDS/PAGE, and immunoblotting was performed by using NR1 monoclonal antibody (Chemicon).

**Biolistic Transfection.** The use of a Gene Gun to propel plasmid DNA-coated gold particles into cells provides a nontoxic and highly efficient method for transfection of neurons in organotypical culture. Preparation of gold micro carriers was performed according to the manufacturer's instruction manual (Bio-Rad), except for the use of polyvinylpyrrolidone (PVP), which was excluded. For each 10 mg of 1.0-$\mu$m gold micro carriers, 12.5 $\mu$g of DNA was used. The Helios gene gun system was set up according to the manufacturer's instructions (Bio-Rad). Transfection of organotypic cultures was performed by using 90 psi helium gas pressure. Cells were cultured for 72 h after transfection before being used. At that time, the D1R-Venus signal was strong in neuronal cells.

**Live Measurements and FRAP.** Live measurements and FRAP are well established methods to study the mobility of proteins (26). Experiments were carried out by using a Zeiss 510LSM laser scanning confocal microscope. A 514-nm laser line was used for both imaging and bleaching. A 40 × 0.8 NA water dipping lens was used; pixel spacing was set to 0.11 $\mu$m. Cells were continuously perfused with magnesium-free physiological phosphate buffer at 37°C. For NMDA exposure, the perfusion solution was switched during 30 s to a solution containing $10^{-3}$ M, $10^{-4}$ M, or $10^{-5}$ M NMDA. The average NMDA concentration during the 30 s of exposure would, however, have been somewhat lower due to dilution in the open recording chamber. We have on a couple of occasions used a fluorescent dye to assess the changes in concentration in our perfusion chamber. We found that the dilution factor was ≈0.5. Exposure to glycine 2 mM was performed in the same way. In live measurements of spines, a 3D stack was recorded for a dendrite of interest during control conditions and 15 min after NMDA exposure. Images were analyzed, and the number of spines on each dendrite was determined by examining all images in the stack. HUYGENS ESSENTIAL 2.6 commercial deconvolution software was used to reduce background noise. For FRAP, dendritic segments 50–150 $\mu$m from the cell body were selected and recorded in a time lapse with one image every 5 s. The first three images were recorded pre-bleach to establish a baseline by using 2% laser power; then, an 8- to 16-$\mu$m-wide region of the dendrite was bleached with 100% laser power for 1–3 s, followed by 57 post-bleach recordings at 2% laser power, 5 min in total. Two separate recordings were performed: the

first was made under control conditions, and the second 3 min after NMDA exposure. In control experiments, both recordings were performed under control conditions. Images were analyzed by using IMAGE EXAMINER (Zeiss) and IMAGEJ (National Institutes of Health). In each experiment, the bleached region was delineated, and the average fluorescence intensity calculated. Data were evaluated both by graphically plotting fluorescence intensities (normalized against the final recovered intensity) and also by fitting to the solution of the diffusion equation.

We thank K. Sugimoto for his work on D1R C terminus phosphorylation. This work was supported by the Swedish Research Council (A.A. and H.B.), the Märta and Gunnar V. Philipson Foundation, Familjen Perssons Stiftelse, and National Institutes of Health Grants MH40899 and DA10044 (to P.G. and A.C.N.).

1. Carlsson, M. L., Carlsson, A. & Nilsson, M. (2004) *Curr. Med. Chem.* **11,** 267–277.
2. Coyle, J. T. (1996) *Harvard Rev. Psychiatry* **3,** 241–253.
3. Scott, L., Kruse, M. S., Forssberg, H., Brismar, H., Greengard, P. & Aperia, A. (2002) *Proc. Natl. Acad. Sci. USA* **99,** 1661–1664.
4. Nagai, T., Ibata, K., Park, E. S., Kubota, M., Mikoshiba, K. & Miyawaki, A. (2002) *Nat. Biotechnol.* **20,** 87–90.
5. Martin-Negrier, M., Charron, G. & Bloch, B. (2000) *Neuroscience* **99,** 257–266.
6. Smiley, J. F., Levey, A. I., Ciliax, B. J. & Goldman-Rakic, P. S. (1994) *Proc. Natl. Acad. Sci. USA* **91,** 5720–5724.
7. Fiorentini, C., Gardoni, F., Spano, P., Di Luca, M. & Missale, C. (2003) *J. Biol. Chem.* **278,** 20196–20202.
8. Maletic-Savatic, M., Malinow, R. & Svoboda, K. (1999) *Science* **283,** 1923–1927.
9. Choquet, D. & Triller, A. (2003) *Nat. Rev. Neurosci.* **4,** 251–265.
10. Lee, F. J., Xue, S., Pei, L., Vukusic, B., Chery, N., Wang, Y., Wang, Y. T., Niznik, H. B., Yu, X. M. & Liu, F. (2002) *Cell* **111,** 219–230.
11. Pei, L., Lee, F. J., Moszczynska, A., Vukusic, B. & Liu, F. (2004) *J. Neurosci.* **24,** 1149–1158.
12. Furukawa, H. & Gouaux, E. (2003) *EMBO J.* **22,** 2873–2885.
13. Laube, B., Schemm, R. & Betz, H. (2004) *Neuropharmacology* **47,** 994–1007.
14. Axelrod, D., Ravdin, P., Koppel, D. E., Schlessinger, J., Webb, W. W., Elson, E. L. & Podleski, T. R. (1976) *Proc. Natl. Acad. Sci. USA* **73,** 4594–4598.
15. Poo, M. M. (1985) *Annu. Rev. Neurosci.* **8,** 369–406.
16. Triller, A. & Choquet, D. (2005) *Trends Neurosci.* **28,** 133–139.
17. Meier, J., Vannier, C., Serge, A., Triller, A. & Choquet, D. (2001) *Nat. Neurosci.* **4,** 253–260.
18. Brakeman, P. R., Lanahan, A. A., O'Brien, R., Roche, K., Barnes, C. A., Huganir, R. L. & Worley, P. F. (1997) *Nature* **386,** 284–288.
19. Changeux, J. P. & Edelstein, S. J. (2005) *Science* **308,** 1424–1428.
20. Tovar, K. R. & Westbrook, G. L. (2002) *Neuron* **34,** 255–264.
21. Kornau, H. C., Schenker, L. T., Kennedy, M. B. & Seeburg, P. H. (1995) *Science* **269,** 1737–1740.
22. Wyszynski, M., Lin, J., Rao, A., Nigh, E., Beggs, A. H., Craig, A. M. & Sheng, M. (1997) *Nature* **385,** 439–442.
23. Kelley, A. E. (2004) *Neuron* **44,** 161–179.
24. Wray, S. (1992) in *Neuromethods 23: Practical Cell Culture Technique*, eds. Boulton, A. A., Baker, G. B. & Walz, W. (Humana, Clifton, NJ), pp. 201–235.
25. Tang, T. S. & Bezprozvanny, I. (2004) *J. Biol. Chem.* **279,** 42082–42094.
26. Lippincott-Schwartz, J., Snapp, E. & Kenworthy, A. (2001) *Nat. Rev. Mol. Cell Biol.* **2,** 444–456.